



Research Paper

Sodium Butyrate Inhibits Inflammation and Maintains Epithelium Barrier Integrity in a TNBS-induced Inflammatory Bowel Disease Mice Model



Guangxin Chen^{a,1}, Xin Ran^{a,1}, Bai Li^{b,1}, Yuhang Li^a, Dewei He^a, Bingxu Huang^a, Shoupeng Fu^a, Juxiong Liu^{a,*}, Wei Wang^{a,*}

^a College of Animal Science and Veterinary Medicine, Jilin University, Changchun, China

^b The First Hospital of Jilin University, Changchun, China

ARTICLE INFO

Article history:

Received 27 February 2018

Received in revised form 23 March 2018

Accepted 26 March 2018

Available online 28 March 2018

Keywords:

GPR109A

SB

TNBS

IBD

Inflammation

Epithelium barrier

ABSTRACT

G Protein Coupled Receptor 109A (GPR109A), which belongs to the G protein coupled receptor family, can be activated by niacin, butyrate, and β -hydroxybutyric acid. Here, we assessed the anti-inflammatory activity of sodium butyrate (SB) on 2,4,6-trinitrobenzene sulfonic acid (TNBS)-induced colitis mice, an experimental model that resembles Crohn's disease, and explored the potential mechanism of SB in inflammatory bowel disease (IBD). *In vivo*, experimental *GPR109a*^{-/-} and wild-type (WT) mice were administered SB (5 g/L) in their drinking water for 6 weeks. The mice were then administered TNBS *via* rectal perfusion to imitate colitis. *In vitro*, RAW246.7 macrophages, Caco-2 cells, and primary peritoneal macrophages were used to investigate the protective roles of SB on lipopolysaccharide (LPS)-induced inflammatory response and epithelium barrier dysfunction. *In vivo*, SB significantly ameliorated the inflammatory response and intestinal epithelium barrier dysfunction in TNBS-induced WT mice, but failed to provide a protective effect in TNBS-induced *GPR109a*^{-/-} mice. *In vitro*, pretreatment with SB dramatically inhibited the expression of TNF- α and IL-6 in LPS-induced RAW246.7 macrophages. SB inhibited the LPS-induced phosphorylation of the NF- κ B p65 and AKT signaling pathways, but failed to inhibit the phosphorylation of the MAPK signaling pathway. Our data indicated that SB ameliorated the TNBS-induced inflammatory response and intestinal epithelium barrier dysfunction through activating GPR109A and inhibiting the AKT and NF- κ B p65 signaling pathways. These findings therefore extend the understanding of GPR109A receptor function and provide a new theoretical basis for treatment of IBD.

© 2018 Published by Elsevier B.V. This is an open access article under the CC BY-NC-ND license (<http://creativecommons.org/licenses/by-nc-nd/4.0/>).

1. Introduction

Inflammatory bowel diseases (IBDs) including Crohn's disease and ulcerative colitis (Baumgart and Sandborn, 2012; Beaugerie et al., 2006) are typically characterized by chronic, progressive, and relapsing inflammation of the intestine. Although the exact pathogenesis of IBD is unknown, it is considered to generally result from multiple immune, genetic, and environmental factors, with only suboptimal medical and surgical therapies being available (Farrell and Peppercorn, 2002). Previous

studies have suggested that although the pathogenesis of ulcerative colitis and Crohn's disease is similar, important differences do exist (Ungaro et al., 2017). Ulcerative colitis is characterized by relapsing and remitting mucosal inflammation, often initiating in the rectum and extending to proximal segments of the colon (Ungaro et al., 2017). However, Crohn's disease constitutes a chronic, relapsing, systemic inflammatory disease that mainly affects the gastrointestinal tract, along with extra-intestinal manifestations and associated immune disorders (Baumgart and Sandborn, 2012).

GPR109A constitutes a G_i protein-coupled receptor that is activated by nicotinic acid (Soga et al., 2003; Tunaru et al., 2003; Wise et al., 2003), butyrate (Thangaraju et al., 2009), and beta-hydroxybutyric acid (Taggart et al., 2005). Previous studies have shown that the activation of GPR109A suppresses mammary tumorigenesis by inducing apoptosis in breast cancer cells (Elangovan et al., 2014). GPR109A is also linked to a pro-apoptotic pathway in neutrophils, suggesting that nicotinic acid may mediate anti-inflammatory effects in addition to its inhibitory function on adipocyte lipolysis (Kostylina et al., 2008). Moreover, as the ligand of GPR109A, niacin acid has the ability to reduce

Abbreviations: Cldn1, claudin-1; DSS, dextran sulfate sodium; FITC, fluorescein isothiocyanate; GPR109A, G Protein Coupled Receptor 109A; IBD, inflammatory bowel disease; LPS, lipopolysaccharide; MUC2, mucin-2; PBS, phosphate buffered saline; SB, sodium butyrate; TNBS, 2,4,6-trinitrobenzene sulfonic acid; WT, wild-type.

* Corresponding authors at: College of Animal Science and Veterinary Medicine, Jilin University, Changchun 130062, China.

E-mail addresses: juxiong@jlu.edu.cn, (J. Liu), wang_wei99@jlu.edu.cn. (W. Wang).

¹ These authors contributed equally to this work.

inflammation in atherosclerosis (Lukasova et al., 2011), obesity (Wanders et al., 2013), sepsis (Kwon et al., 2011), diabetic retinopathy (Gambhir et al., 2012), renal disease (Cho et al., 2009), and Parkinson's disease (Fu et al., 2014; Fu et al., 2015). Together, these findings indicated that GPR109A has the ability to inhibit inflammation in various diseases. In particular, studies have reported that the GPR109A receptor mediates the protective effects of dietary fiber on gut homeostasis through regulation of the inflammasome in dextran sulfate sodium (DSS)-induced mice (Macia et al., 2015) and suppresses colonic inflammation and tumorigenesis in mice (Singh et al., 2014; Thangaraju et al., 2009). However, the mechanism underlying GPR109A mediation of the process by which butyric acid inhibits inflammation and maintains epithelial barrier integrity in inflammatory bowel disease has not yet been elucidated.

Butyrate, which is produced by bowel microbial fermentation of dietary carbohydrates, fibers, proteins, and peptides (Guilloteau et al., 2010; Leonel and Alvarez-Leite, 2012; Macfarlane and Macfarlane, 2003), serves as the energy source of small intestinal epithelial cells (Chen et al., 2015), thus stimulating their growth (Guilloteau et al., 2010). In this study, mice (*in vivo*) and cells (*in vitro*) were pre-treated with sodium butyrate (SB), a ligand of GPR109A, to explore the anti-inflammatory effects and functional mechanism of the GPR109A receptor.

2. Materials and Methods

2.1. Animals and Models

For all experiments, we utilized 6–8-week-old male *GPR109a*^{-/-} and wild-type (WT) C57BL/6 mice. The *GPR109a*^{-/-} is whole body KO which was a generous gift from Dr. Martin Sager (Zentrale Einrichtung für Tierforschung und Tierschutzaufgaben der Heinrich-Heine Universität Düsseldorf, Germany). The WT mice were provided by the Centre of Experimental Animals of the Baiqiu Medical College of Jilin University (Changchun, China). Mice were housed at 22–23 °C, with a 12 h/12 h light/dark cycle, and *ad libitum* access to food and water. The experiments were approved by the Jilin University Institutional Animal Care and Use Committee. For the 2,4,6-trinitrobenzene sulfonic acid (TNBS) model, colitis was induced by intracolonic administration of TNBS, as previously described (Piekielna et al., 2012). Briefly, mice were lightly anesthetized *via* inhalation of diethyl ether. Then, 3.5 mg of TNBS in the 100 µL of 30% ethanol solution was administered into the colon through a catheter inserted approximately 3 cm into the anus.

2.2. Experimental Groups

Mice were randomly assigned to six groups, each containing 14 mice. Sham-WT and Sham-*GPR109a*^{-/-} were used as the normal control groups, TNBS-WT, and TNBS-*GPR109a*^{-/-} comprised the TNBS treatment groups, and SB-TNBS-WT and SB-TNBS-*GPR109a*^{-/-} included

mice that were first administered SB *via* their drinking water for 6 weeks before being treated with TNBS.

2.3. Disease Activity Index

During the experiment, body weight, stool character and fecal occult blood were recorded. The disease activity index (DAI) was calculated based on the scoring system as shown in Table 1 as previously described (Murano et al., 2000).

Score	Weight loss (%)	Stool character	Fecal occult blood
0	0	Normal formed	Negative
1	1–5%		
2	5–10%	Loose stool	Positive
3	10–20%		
4	>20%	Diarrhea	Gross bleeding

2.4. Hematoxylin and Eosin (H&E)-Staining and Immunofluorescence

Colonic segments (approximately 2–3 cm long) were excised, washed in phosphate buffered saline (PBS), fixed in 4% formaldehyde, embedded in paraffin, and sectioned (5 µm). One set of paraffin sections was stained with H&E, and the total damage score was determined based on the goblet cell depletion (presence = 1, absence = 0), crypt abscesses (presence = 1, absence = 0), mucosal architecture destruction (normal = 1, moderate = 2, extensive = 3), muscle thickening (normal = 1, moderate = 2, extensive = 3), and cellular infiltration (normal = 1, moderate = 2, transmural = 3). The remaining sections were used for immunofluorescence; detailed procedures can be found in Schaubek et al. (2016). Briefly, antigens were unmasked by boiling under pressure in sodium citrate buffer. Sections were cooled to room temperature (approximately 25 °C) naturally, then washed three times (5 min each time) with PBS. Sections were then incubated with a blocking buffer (5% donkey serum and 0.1% Triton X-100 in PBS) against the species of the secondary antibody for 60 min. Primary antibodies were incubated at 4 °C overnight, and then washed three times with PBS. Secondary antibodies were diluted to 1:1000, incubated for 1 h at room temperature, and then washed three times in PBS. Nuclei were counterstained using DAPI.

2.5. *In vivo* Intestinal Permeability Assay

Intestinal permeability was evaluated using fluorescein isothiocyanate (FITC)-dextran with an average molecular weight of 3000–5000 (Sigma-Aldrich, St. Louis, MO), as previously described (Jeong et al., 2016). Briefly, 2 days after TNBS treatment, mice were starved for 4 h and then gavaged with FITC-dextran (0.6 mg/g body weight at a concentration of 125 mg/mL). After 4 h, blood was collected from the eyes of the mice and centrifuged at 12,000g for 3 min. The FITC-dextran content in serum was determined using a microplate reader with

Table 1
Primers used for qRT-PCR.

Gene	Primer sequence
<i>Tnfa</i>	F: 5'-GCAACTGCTGCACGAAATC-3'
<i>Il6</i>	F: 5'-CCAGAAACCGCTATGAAGTTC-3'
<i>Cldn1 (mou)</i>	F: 5'-AGGTCTGGCGACATTAGTGG-3'
<i>Ocln (mou)</i>	F: 5'-ACACTTGCTGGGACAGAGG-3'
<i>Zo1 (mou)</i>	F: 5'-GACCTTGATTGCATGACGA-3'
<i>CLDN1 (hum)</i>	F: 5'-CCCTTGATCCCTACCAACA-3'
<i>OCLN (hum)</i>	F: 5'-ATGGCTGCCTTTTGTTCAT-3'
<i>ZO1 (hum)</i>	F: 5'-CTCCTGGATTGGATTGGA-3'
<i>β-actin (mou)</i>	F: 5'-GTCAGGTCATCACTATCGCAAT-3'
<i>GAPDH (hum)</i>	F: 5'-CTCTGGATTGGATTGGA-3'
	R: 5'-CTGCTTGTCTCTGCCAC-3'
	R: 5'-GTTGGGAGTGGTATCTCTGTGA-3'
	R: 5'-CGTGGTGTGGGTAAGAGGT-3'
	R: 5'-AAGGAAGCGATGAAGCAGAA-3'
	R: 5'-AGGACCGTGAATGGCAGAC-3'
	R: 5'-CAGGACAGGAACAGGAGAGC-3'
	R: 5'-ATGCCAGGATAGCACTAC-3'
	R: 5'-CTGCTTCAGCTGGTCTC-3'
	R: 5'-AGAGGCTTTACGGATGCAACGT-3'
	R: 5'-CTGCTTCAGCTGGTCTC-3'

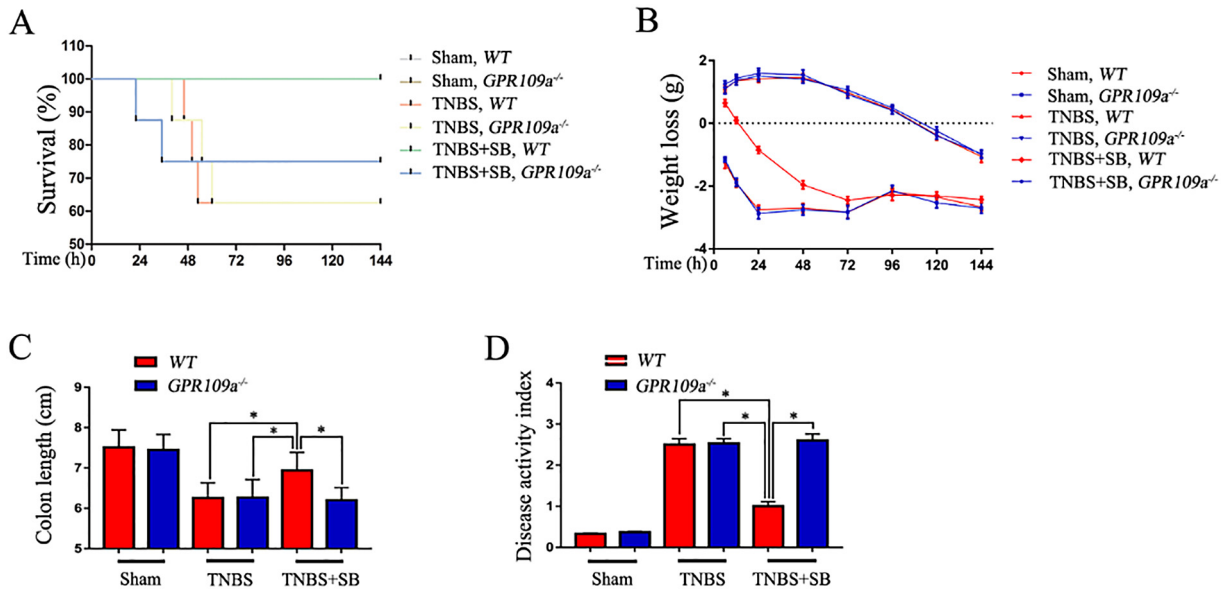


Fig. 1. SB ameliorates survival, weight loss, colon length, and disease activity index in the TNBS-induced mouse IBD model. WT and *GPR109a*^{-/-} mice were pre-treated with SB for 6 weeks and then treated with TNBS for 6 days. (A) Survival of TNBS- and SB-treated WT and *GPR109a*^{-/-} mice (n = 14). (B) Weight loss (the previous day's body weight – the day's body weight) in TNBS- and SB-treated WT and *GPR109a*^{-/-} mice (n = 8–12). (C) Colon length in TNBS- and SB-treated WT and *GPR109a*^{-/-} mice (n = 8–12). (D) Disease activity index of TNBS- and SB-treated WT and *GPR109a*^{-/-} mice (n = 8–12).

excitation and emission wavelengths of 490 and 525 nm, respectively. Each sample was measured in triplicate.

2.6. Cell Culture

Caco-2 cells and RAW246.7 macrophages, purchased from BeNa Culture Collection (Beijing, China), were cultured in Dulbecco's modified

Eagle's medium (Gibco, Grand Island, NY) containing 10% fetal bovine serum (Clark, Australia) and were maintained at 37 °C in a humidified chamber of 5% CO₂.

The mice were intraperitoneally injected with 4 mL of 3% thioglycollate broth. After three days, the mice were sacrificed and then each mouse was injected with 4 mL RPMI 1640 into the peritoneal cavity. The peritoneal lavage fluid was collected and centrifuged at 300g

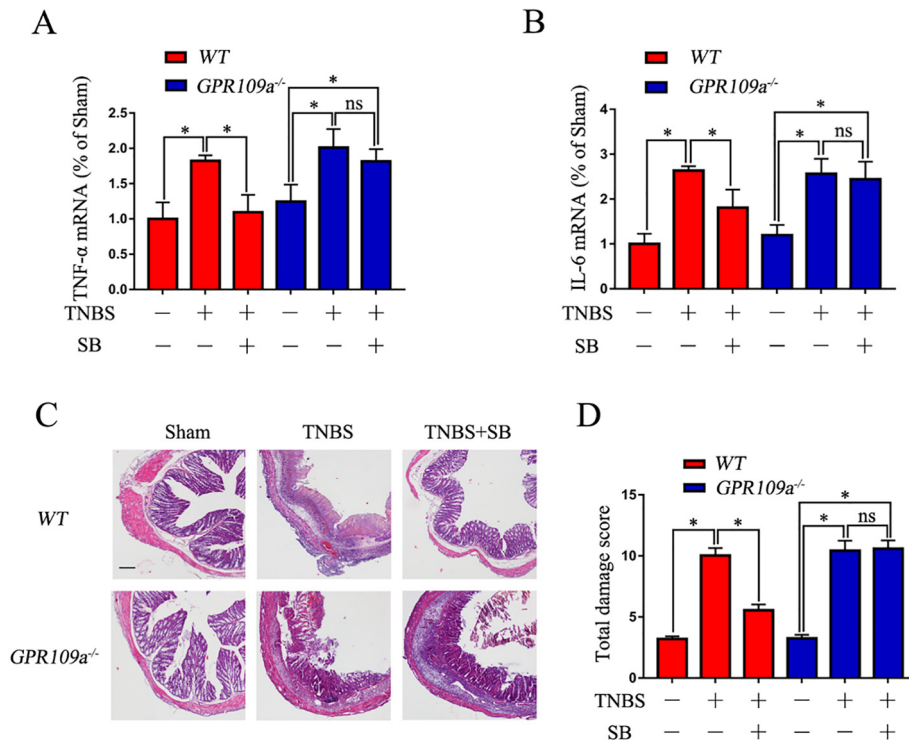


Fig. 2. SB suppresses the inflammation in TNBS-induced mice. (A–B) Expression of the pro-inflammatory cytokines TNF-α and IL-6 in colon tissue homogenate (n = 4). (C) H&E staining of colon tissue from TNBS- and SB-treated WT and *GPR109a*^{-/-} mice, magnification shown is 4 ×, and the scale bar represents 100 μm (n = 4). (D) Total damage score of TNBS- and SB-treated WT and *GPR109a*^{-/-} mice (n = 8–12).

for 5 min. The supernatant was removed and the cells were re-suspended in RPMI 1640 medium supplemented with 10% fetal bovine serum and maintained at 37 °C with 5% CO₂. After 2 h, non-adherent cells were discarded. The remaining adherent cells were cultured overnight until they were used for the experiments.

2.7. Trans Epithelial Electric Resistance

The Caco-2 cells were seeded in Transwell cell culture chambers (6.5-mm diameter inserts, 3.0 μm pore size) (Corning Costar, Cambridge, MA) and cultured for 11 days to form a cell monolayer. Then, RAW246.7 macrophages were seeded in the bottom of the well. After three days, the RAW246.7 macrophages were pre-treated with SB (5 mM) for 1 h and then stimulated with lipopolysaccharide (LPS) (1 μg/mL) for 24 h, as shown in Fig. 5A. The complete medium was replaced with serum free medium and incubated for 20 min, and then the TEER value was measured using a resistor:

$$\text{TEER} = \frac{R - \text{RB}}{\text{Surface Area}} (\Omega/\text{cm}^2)$$

Where R is the resistance of the cell monolayer along with the filter membrane, RB is the resistance of the filter membrane (black), and Surface Area = (0.65 cm ÷ 2)² × 3.14 = 0.332 cm².

2.8. Cell Co-Culture

The RAW246.7 macrophages and Caco-2 cells were seeded in 6-well plates and cultured for 48 h. Then, the RAW246.7 macrophages were stimulated with LPS for 12 h. The medium supernatant was collected and centrifuged at 12,000 g for 10 min to remove cell debris. The collected medium supernatant was used to stimulate the Caco-2 cells for 12 h, as shown in Fig. 5C. The Caco-2 cells were collected to measure the expression of the tight junction encoding genes claudin-1 (*Cldn1*), occludin (*Ocln*), and *Zo1* using qRT-PCR.

2.9. RNA Extraction, Complementary DNA (cDNA) Preparation, and Real-time Reverse Transcription-Polymerase Chain Reaction (RT-PCR)

Total RNA was extracted from the colon tissue, RAW246.7 macrophages, Caco-2 cells, and primary peritoneal macrophages using TRIzol (Invitrogen, Carlsbad, CA), and cDNA was generated using a commercial RT-PCR kit (TaKaRa Shuzo Co., Ltd., Kyoto, Japan). Then, real-time PCR was conducted using the SYBR Green QuantiTect RT-PCR kit (Roche, South San Francisco, CA), and each of the samples was analyzed in triplicate. The sequences of the primers used in this investigation are shown in Table 1.

2.10. Western Blotting

RAW246.7 cells and primary peritoneal macrophages were treated with SB (5 mM) for 1 h, and treated with LPS (1 μg/mL) for 2 h. Then, the cells were lysed with a lysis buffer (Beyotime Inst. Biotech, Beijing, China). The protein concentrations in the supernatants were quantified using a bicinchoninic acid protein assay kit (Beyotime Inst. Biotech), and 30 μg of protein was resolved by 10% sodium dodecyl sulfate-polyacrylamide gel electrophoresis and transferred to immunoblot polyvinylidene difluoride membranes (Millipore, Billerica, MA). The membranes were blocked with 5% non-fat milk in Tris-buffered saline with 0.1% Tween (TBS-T) for 1 h, washed four times in TBS-T, followed by overnight incubation at 4 °C with primary antibodies against p-p38 (1:2000), p-38 (1:2000), p-JNK1/2 (1:2000), JNK1/2 (1:2000), p-ERK1/2 (1:2000), ERK1/2 (1:2000), p-AKT (1:2000), AKT (1:2000), p-NF-κB p65 (1:2000), NF-κB p65 (Cell Signaling Technology, Danvers, MA), and β-actin (1:2000) (Santa Cruz Technologies, Dallas, TX). Then, the membranes were again washed four times with TBS-T

(15 min each time) and incubated with a horseradish peroxidase-labeled secondary goat anti-rabbit (1:2000; Santa Cruz Technologies) or rabbit anti-goat (1:2000; Santa Cruz Technologies) antibody for 1 h at room temperature. Next, the blots were washed again four times with TBS-T (15 min each time). Membranes were visualized using enhanced chemiluminescence (ECL kit; Applygen Inst. Biotech, Beijing, China).

2.11. Statistics

Results are expressed as the means ± SE. Data were analyzed using the statistical software package SPSS 12.0 (SPSS Inc., Chicago, IL). Groups were compared by one-way analysis of variance (ANOVA) followed by the least significant difference test. **P* < 0.05 was considered significant, and ***P* < 0.01 was considered markedly significant.

3. Results

3.1. SB Ameliorates Survival, Weight Loss, Colon Length, and Clinical Scores in a TNBS-Induced Mouse IBD Model

Initially, to define whether SB has a protective role in colitis *in vivo*, a series of indices were measured in TNBS-induced mice. First, we tested the survival of TNBS-induced WT and *GPR109a*^{-/-} mice and found no significant difference. Pre-treatment with SB for 2 months observably improved the WT mouse survival rate; however, the effect was not observed in *GPR109a*^{-/-} mice (Fig. 1A). Next, we measured the weight loss (initial weight – real time weight) and found that TNBS decreased the weight of WT and *GPR109a*^{-/-} mice, whereas SB increased the body weight of WT mice but had no effect on *GPR109a*^{-/-} mice (Fig. 1B). TNBS decreased the colon length in WT and *GPR109a*^{-/-} mice, whereas pre-treatment with SB increased the colon length in WT mice but not in *GPR109a*^{-/-} mice (Fig. 1C). Lastly, we found that TNBS significantly increased the disease activity index in WT and *GPR109a*^{-/-} mice, and SB decreased the disease activity index in WT mice (Fig. 1D). Together, these results indicated that SB plays a GPR109A-dependent protective role in TNBS-induced colitis.

3.2. SB Suppresses Inflammation in TNBS-Induced Mice

The qRT-PCR results showed that TNBS significantly increased the expression of TNF-α and IL-1β in colon tissue homogenates of WT and *GPR109a*^{-/-} mice; however, pre-treatment with SB strikingly decreased their expression in WT but not in *GPR109a*^{-/-} mice (Fig. 2A,B). Evaluation of the severity of colonic inflammation and ulceration by histopathological examination showed marked infiltration of inflammatory cells, loss of crypts, destruction of the mucosal layer, and edema in TNBS-induced WT and *GPR109a*^{-/-} mice. In contrast, the colons of WT mice pre-treated with SB showed only mild inflammation; however, SB had no effects on TNBS-induced *GPR109a*^{-/-} mice (Fig. 2C). The protective effects of SB on TNBS-induced mice were also observed in total damage score (Fig. 2D). The results indicated that SB suppressed the inflammation in TNBS-induced mice in a GPR109A-dependent manner.

3.3. SB Reduces the Permeability and Maintains Proper Tight Junctions and Mucin-2 in TNBS-Induced Mice

SB decreased the intestinal permeability in TNBS-induced WT mice; however, SB had no effects in TNBS-induced *GPR109a*^{-/-} mice (Fig. 3A). qRT-PCR assessment of *Cldn1*, *Zo1*, and *Ocln* mRNA expression showed that their expression was reduced in TNBS-induced WT and *GPR109a*^{-/-} mice, whereas supplementation with SB precluded this effect in TNBS-induced WT but not *GPR109a*^{-/-} mice (Fig. 3C-E). Immunofluorescence-mediated examination of mucin-2 (MUC2) protein expression showed that

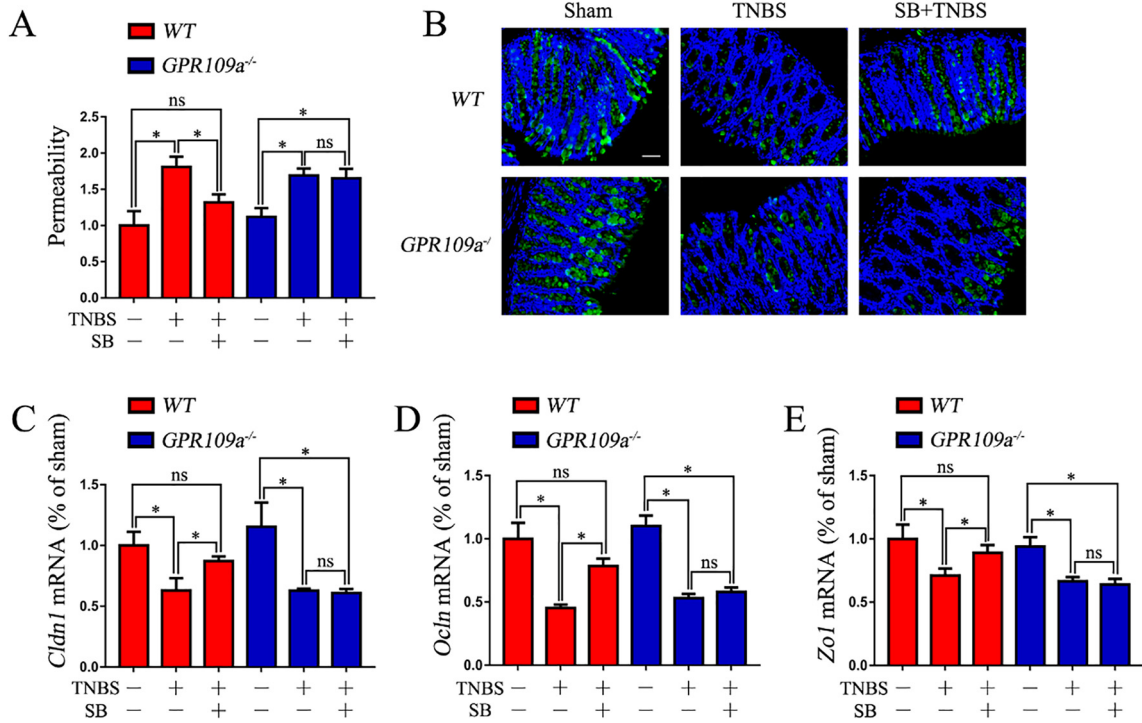


Fig. 3. SB reduces the permeability and maintains proper tight junctions and mucin-2 in TNBS-induced mice. All mice were pre-treated with SB for 6 weeks, and then treated with TNBS for 2 days. (A) Relative permeability of TNBS and SB treatment in WT and *GPR109a*^{-/-} mice. After treating with SB and TNBS, the mice were starved for 4 h and then gavaged with FITC-dextran (0.6 mg/g body weight at a concentration of 125 mg/mL). Serum from blood collected after 4 h was used to measure the permeability (n = 4). (B) Immunofluorescence staining of Muc2 in the colon; magnification shown is 10 ×, and the scale bar represents 300 μm (n = 4). (C-E) Expression of the tight junction encoding genes *Cldn1*, *Ocln*, and *Zo1* in the colon tissue homogenate of TNBS- and SB-treated WT and *GPR109a*^{-/-} mice (n = 4).

MUC2 was reduced in both TNBS-induced WT and *GPR109a*^{-/-} mice. WT mice maintained proper MUC2 protein expression when supplemented with SB, but no improvement was observed in

GPR109a^{-/-} mice (Fig. 3B). Together, these results indicated that SB reduced the permeability and maintained proper tight junctions and mucin-2 by activating GPR109A in TNBS-induced mice.

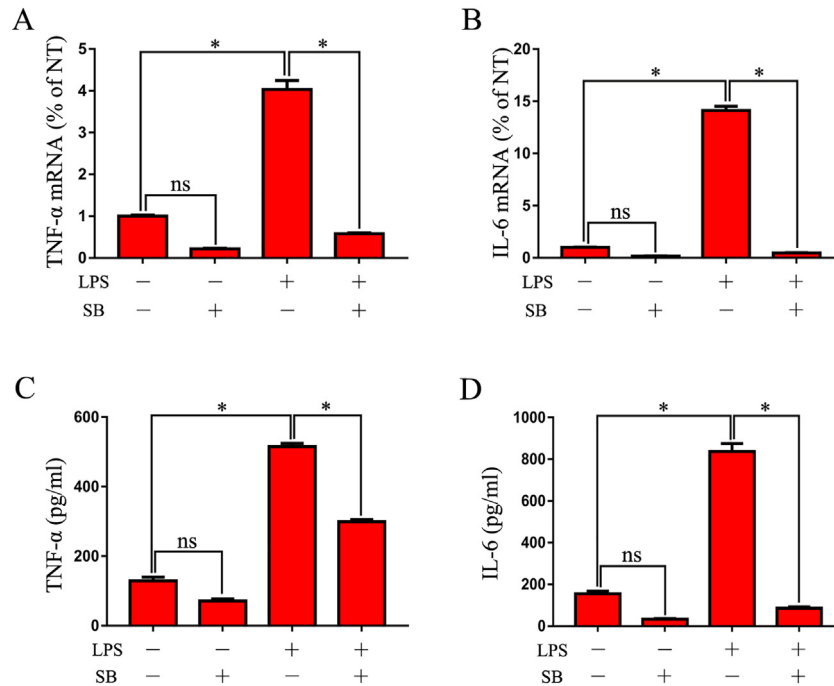


Fig. 4. SB suppresses pro-inflammatory cytokine expression in LPS-induced macrophages. (A-B) Expression of TNF-α and IL-6 in SB- and LPS-treated RAW246.7 cells. RAW246.7 macrophages were stimulated with LPS for 6 h after pre-treating with SB for 1 h, and then the cells were collected with TRIzol. Gene expression of TNF-α and IL-6 was detected by qRT-PCR (n = 3). (C-D) Protein levels of TNF-α and IL-6 in the medium supernatant of SB- and LPS-treated RAW246.7 macrophages. RAW246.7 macrophages were pre-treated with SB for 1 h, and then stimulated with LPS for 12 h. The medium supernatant was collected and used for measuring the protein levels of TNF-α and IL-6 by ELISA (n = 3).

3.4. SB Suppresses Pro-Inflammatory Cytokine Expression in LPS-Induced Macrophages

qRT-PCR assessment of *in vitro* pro-inflammatory cytokine expression showed that TNF- α and IL-6 expression increased in 6-h-LPS-induced RAW246.7 cells. However, pre-treatment with SB sharply decreased the expression of pro-inflammatory mediators (Fig. 4A, B). In comparison, ELISA measurement of the levels of the pro-inflammatory cytokines in the supernatant of 12-h-LPS-induced RAW246.7 cells showed that SB pretreatment markedly inhibited the release of TNF- α and IL-6 (Fig. 4C, D).

3.5. SB Maintains a Proper Intestinal Epithelium Barrier by Inhibiting the Inflammatory Response of Macrophages

To investigate the protective role of SB on the intestinal epithelium barrier *in vitro*, we simulated the intestinal physiological environment by culturing Caco-2 and RAW 246.7 cells together in a Transwell® plate (Fig. 5A). The results showed that LPS significantly decreased the resistance of the monolayer, whereas pre-treating with SB observably inhibited this reducing effect (Fig. 5B). Next, we also performed a co-

culture experiment to confirm whether the protective effects of SB on the intestinal epithelium barrier occurred by inhibiting the inflammatory response of macrophages. The results showed that the medium supernatant of LPS-stimulated but not SB plus LPS-treated RAW246.7 macrophages significantly decreased the expression of *Cldn1*, *Zo1*, and *Ocln* (Fig. 5 C-F). Together, the results indicated that SB maintained the proper epithelium barrier by inhibiting the secretion of pro-inflammatory mediators from macrophages.

3.6. SB Suppresses LPS-Induced Phosphorylation of the AKT and NF- κ B p65 Signaling Pathways in Macrophages

LPS sharply improved the phosphorylation of p-38, JNK1/2, ERK1/2, AKT, and NF- κ B p65 signaling pathways in RAW246.7 cells (Fig. 6A, E), whereas SB pre-treatment significantly inhibited the phosphorylation of AKT and NF- κ B p65 (Fig. F, G), but not p-38, JNK1/2, and ERK1/2 in LPS-induced RAW246.7 macrophages (Fig. 6B-D). SB also clearly inhibited the phosphorylation of AKT and NF- κ B p65 in LPS-induced WT mouse primary peritoneal macrophages (Fig. 6H-J), but failed to inhibit this phenomenon in LPS-induced *GPR109a*^{-/-} mouse primary peritoneal macrophages (Fig. 6K-M).

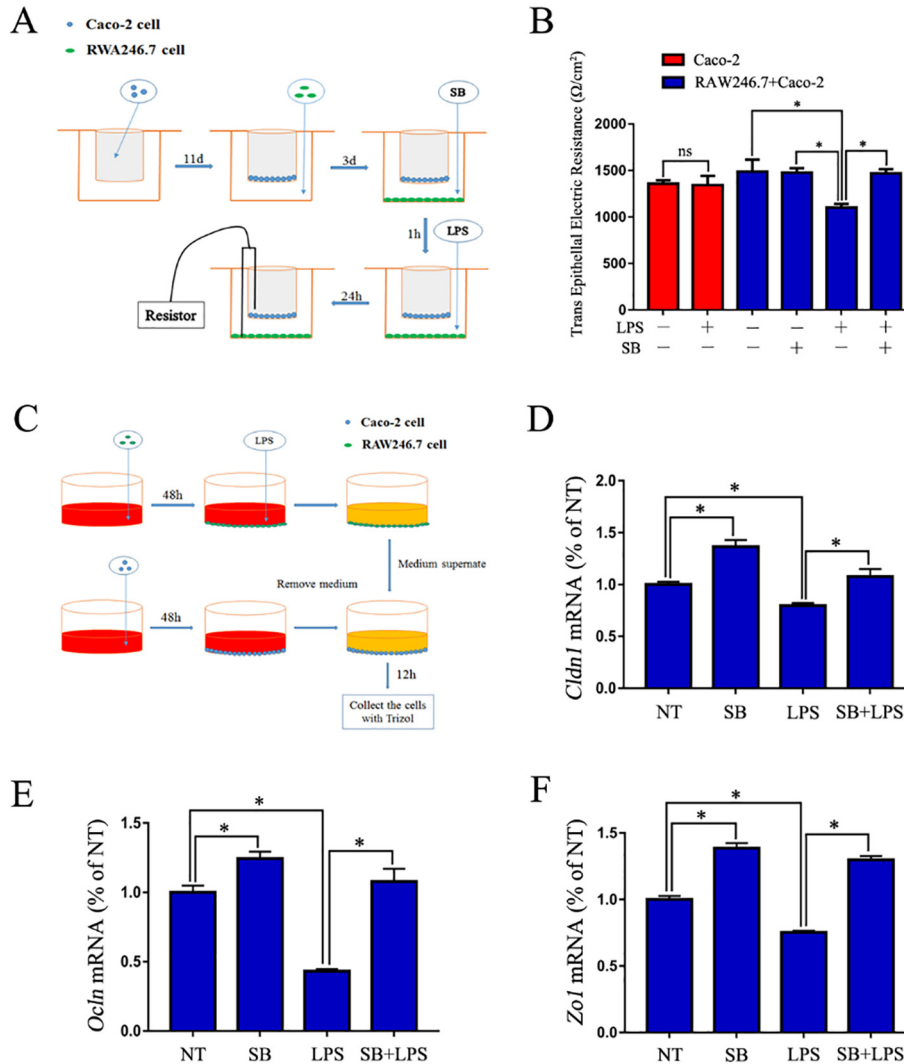


Fig. 5. SB maintains a proper intestinal epithelium barrier by inhibiting the inflammatory response of macrophages. (A) Schematic diagram of the testing process of TEER. (B) TEER of various treatments of the Caco-2 monolayer (n = 3). (C) Schematic diagram of Caco-2 cell and RAW246.7 macrophage co-culture. (D-E) Expression of the tight junction genes *Cldn1*, *Ocln*, and *Zo1* of Caco-2 cells (n = 3).

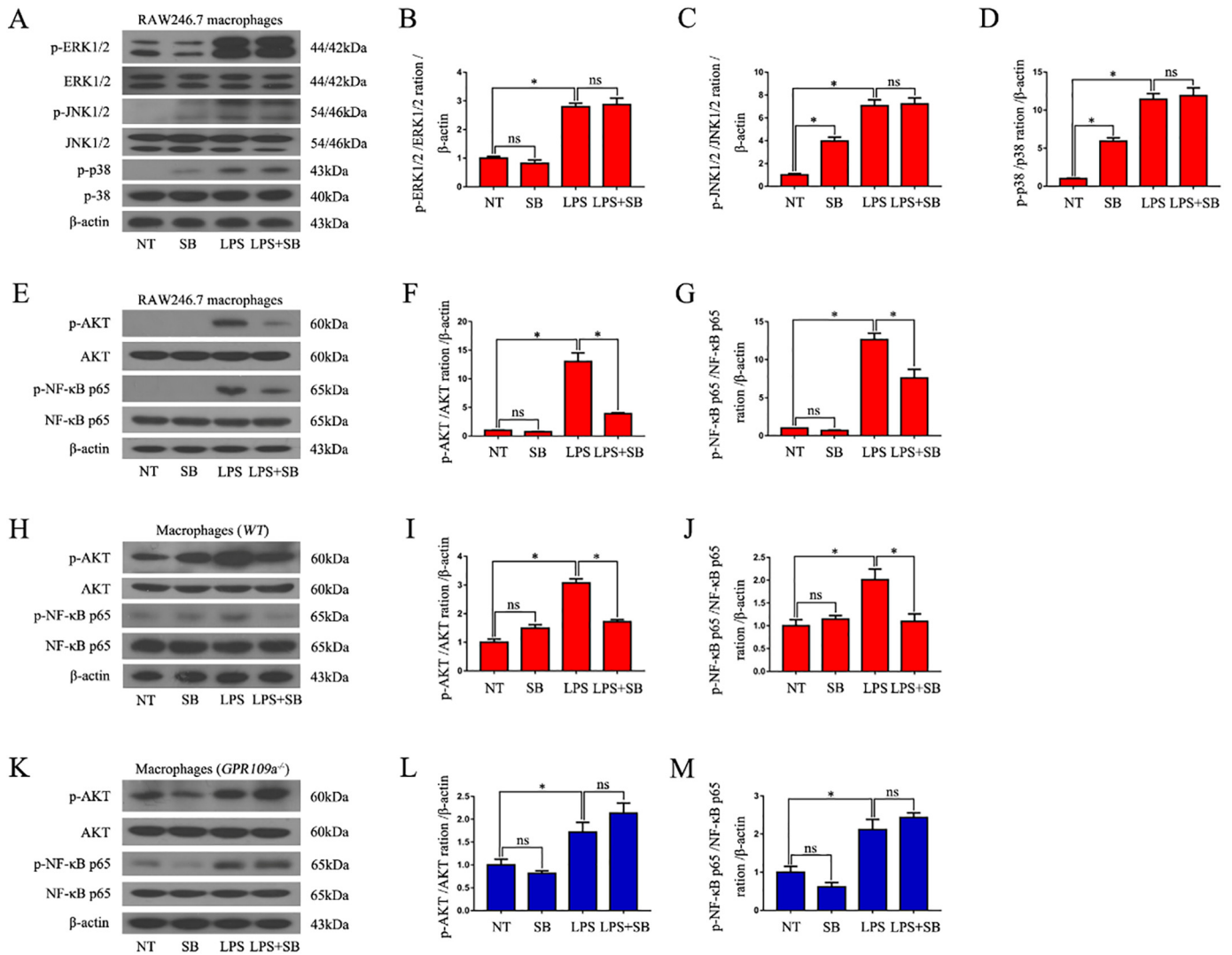


Fig. 6. SB suppresses LPS-induced phosphorylation of the AKT and NF- κ B p65 signaling pathways in macrophages. (A–G) Western blot analysis of the phosphorylation of the p38, ERK p-38, JNK1/2, ERK1/2, AKT, and NF- κ B p65 signaling pathways in LPS-induced RAW246.7 macrophages ($n = 3$). (H–J) Western blot analysis of the phosphorylation of the AKT and NF- κ B p65 signaling pathways in LPS-induced WT mouse primary peritoneal macrophages ($n = 3$). (K–M) Western blot analysis of the phosphorylation of the AKT and NF- κ B p65 signaling pathways in LPS-induced *GPR109a*^{-/-} mouse primary peritoneal macrophages ($n = 3$).

4. Discussion

A growing body of evidence suggests that the activation of GPR109A suppresses the inflammatory effects in various diseases (Rahman et al., 2014; Sivaprakasam et al., 2016; Xu et al., 2017; Yang et al., 2015). Additionally, previous studies showed that the activation of GPR109a inhibits the inflammation seen in IBD (Salem and Wadie, 2017; Singh et al., 2014). However, these reports all focused on the anti-inflammatory effects of GPR109a and ignored the potential protective effects of GPR109A on the impaired intestinal epithelium barrier. Butyrate is produced by the intestinal microbial fermentation of dietary carbohydrates, fiber, proteins, and peptides (Guilloteau et al., 2010; Leonel and Alvarez-Leite, 2012). SB has been reported to decrease post-weaning diarrhea by modulating intestinal permeability in weaned piglets (Huang et al., 2015), promoting the recovering of intestinal wound healing through its positive effect on the tight junctions (Ma et al., 2012) and butyrate-releasing derivatives maintain proper *Zo1* and *Ocln* expression in the colons of patients with DSS-induced colitis (Simeoli et al., 2017). However, the effect of SB on impaired intestinal epithelium barriers is not clear. In the present study, we examined the anti-inflammatory property of SB; confirmed its potential protective roles on the impaired intestinal epithelium barrier in a TNBS-induced IBD mouse model; and explored its

mechanism in RAW246.7 macrophages, Caco-2 cells, and primary peritoneal macrophages *in vitro*.

Depressed survival rate, body weight, and colon length along with elevated clinical score comprise the essential characteristics of IBD (Hung et al., 2014; Shen et al., 2011; Sun et al., 2010). In the present study, we found that SB improved the survival rate, body weight, and colon length and decreased the clinical score in TNBS-induced WT mice, but had no effects on *GPR109a*^{-/-} mice. We also found that supplementation with SB markedly inhibited the inflammatory response in TNBS-induced mice and LPS-induced macrophages. The results are consistent with previous reports that activation of the GPR109A receptor provides a protective effect on IBD (Macia et al., 2015; Singh et al., 2014). Dietary fiber exhibits multiple beneficial effects toward the maintenance of intestinal homeostasis, which are believed to be due to the fermentation of fibers by intestinal microbiota, resulting in the production of short-chain fatty acids such as acetate, propionate, and butyrate (Koh et al., 2016). Among the short-chain fatty acids, butyrate has attracted more attention, being shown to function as an energy source for colonocytes, to exhibit anti-inflammatory as well as immune modulatory effects, and to protect against intestinal cancer in a GPR109A-dependent manner (Koh et al., 2016; Leonel and Alvarez-Leite, 2012; Offermanns, 2017). Therefore, our results are consistent with those of

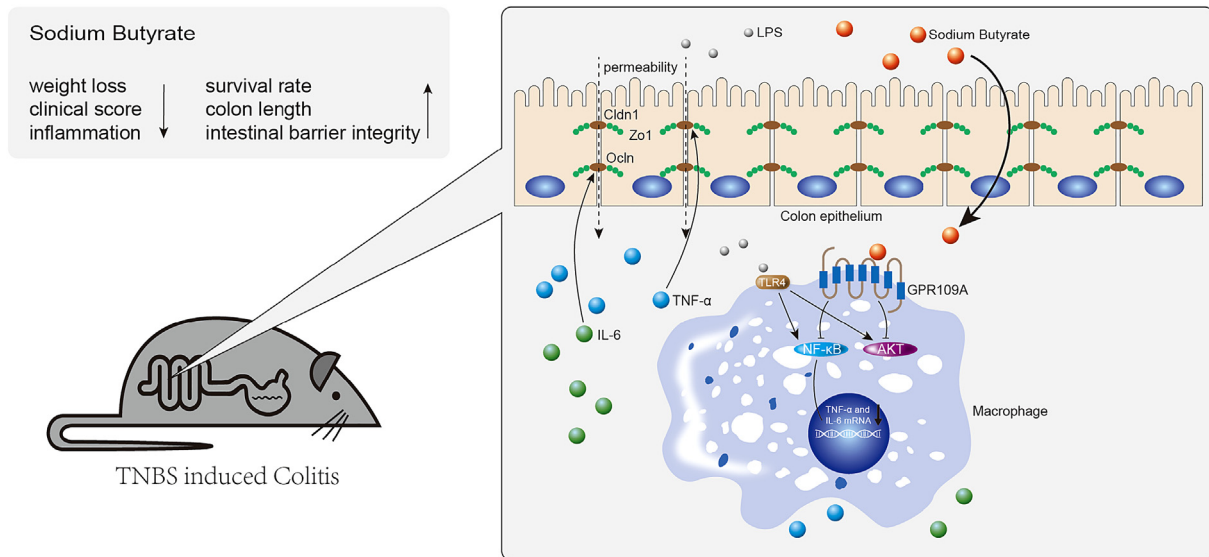


Fig. 7. Mechanism of sodium butyrate on inhibiting inflammation and maintaining epithelium barrier integrity in the TNBS-induced colitis model.

previous studies wherein supplementation with fiber improves DSS- or TNBS-induced mouse colitis (Macia et al., 2015; Oppong et al., 2015), quite possibly in a GPR109A-dependent manner.

The intestinal epithelium, among the most important interfaces between the body and the environment, not only plays a part in nutrient absorption but also acts as a barrier against the vast amount of commensal intestinal microorganisms and pathogenic microbes (Artis and Grencis, 2008; Peterson and Artis, 2014). Therefore, the integrity of the epithelial monolayer is critical for the health of the gut, and epithelial dysfunction is a hallmark of intestinal disorders such as IBDs (Citalan-Madrid et al., 2017; Worthington et al., 2017). In the TNBS-induced murine colitis model, ethanol is essential for providing access to intestinal epithelial cells, impairing barrier function, and allowing TNBS to penetrate the bowel wall. TNBS constitutes a covalently reactive compound that attaches to autologous proteins and stimulates a delayed-type hypersensitivity response to hapten-modified self antigens, a reaction that involves and is regulated by complex interactions among various functional subsets of CD4⁺ T cells (Elson et al., 1996; Miller and Butler, 1983), subsequently leading to the inflammatory response of innate immune cells and further damage of the intestinal epithelium barrier. In the present study, we found that SB reduced the permeability of the intestine and maintained proper tight junctions and MUC2 in the colon of TNBS-induced *WT* mice. To further confirm these results, we examined the effects of SB on the epithelium barrier *in vitro* and found that SB sharply reduced the effects of LPS-induced RAW246.7 macrophages on the resistance of the Caco-2 cell monolayer, as well as maintained proper tight junctions. Together, these results indicated that SB maintained a proper intestinal epithelium barrier by activating GPR109A.

A previous study indicated that GPR109a mediates the anti-inflammatory effect by inhibiting the phosphorylation of the NF- κ B p65 signaling pathway (Fu et al., 2015; Zandi-Nejad et al., 2013). In the present study, to investigate the definite mechanism of SB on the inflammatory response, we examined the effects of SB on the classical inflammation pathways AKT, NF- κ B, and MAPK and found that supplementation with SB markedly decreased the phosphorylation of AKT and NF- κ B p65 in LPS-induced RAW246.7 cells and *WT* mouse primary peritoneal macrophages, but failed to suppress this phenomenon in *GPR109a*^{-/-} mouse primary peritoneal macrophages. Previous studies indicated that supplementation with SB improved the phosphorylation of the AKT signaling pathway in high-fat diet-induced insulin resistance

(Gao et al., 2009; Zhang et al., 2017), elevated the phosphorylation of the AKT signaling pathway in the adipose tissue of obese mice (Guo et al., 2017), and inhibited platelet-derived growth factor-induced proliferation and migration in pulmonary artery smooth muscle cells through AKT inhibition (Cantoni et al., 2013). Therefore, the effects of SB on the AKT signaling pathway are not fixed; instead, they depend on the function of the AKT signaling pathway in different situations. Our results indicated that SB inhibited the phosphorylation of the AKT and NF- κ B p65 signaling pathway in macrophages in a GPR109A-dependent manner.

Fig. 7 summarizes the underlying mechanism of SB on inhibiting inflammation and maintaining epithelium barrier integrity in the TNBS-induced colitis model. Our findings not only explained the protective effect of SB on colon health, but also provided evidence that GPR109A likely constitutes a valid therapeutic target in IBD. Inhibition of macrophages by activating GPR109A thus may represent a novel approach to treat IBD.

Acknowledgments

We are grateful to Dr. Martin Sager (Zentrale Einrichtung für Tierforschung und Tierschutzaufgaben der Heinrich-Heine Universität Düsseldorf, Germany) for providing the *GPR109a*^{-/-} mice (whole body KO). We would like to thank WebShop (www.webshop.elsevier.com) for English language editing.

Funding

This study was supported by National Nature Science Foundation of China (31572479, 31702211, 31602020) and Graduate Innovation Fund (2017168) of Jilin University.

Conflict of Interest Statement

The authors declare no conflict of interest.

Author Contributions

WW and JXL provided the initial concept and managed the study. GXC, XR, and BL performed the majority of the experiments and collected the data. YHL performed the qRT-PCR. DWH, BXH, and SPF performed the western blotting. GXC and WW wrote the initial draft of the manuscript.

Reference

- Artis, D., Grencis, R.K., 2008. The intestinal epithelium: sensors to effectors in nematode infection. *Mucosal Immunol.* 1, 252–264.
- Baumgart, D.C., Sandborn, W.J., 2012. Crohn's disease. *Lancet* 380, 1590–1605.
- Beaugerie, L., Seksik, P., Nion-Larmurier, I., Gendre, J.P., Cosnes, J., 2006. Predictors of Crohn's disease. *Gastroenterology* 130, 650–656.
- Cantoni, S., Galletti, M., Zambelli, F., Valente, S., Ponti, F., Tassinari, R., Pasquinelli, G., Galie, N., Ventura, C., 2013. Sodium butyrate inhibits platelet-derived growth factor-induced proliferation and migration in pulmonary artery smooth muscle cells through Akt inhibition. *FEBS J.* 280, 2042–2055.
- Chen, J., Li, Y., Tian, Y., Huang, C., Li, D., Zhong, Q., Ma, X., 2015. Interaction between microbes and host intestinal health: modulation by dietary nutrients and gut-brain-endocrine-immune axis. *Curr. Protein Pept. Sci.* 16, 592–603.
- Cho, K.H., Kim, H.J., Rodriguez-Iturbe, B., Vaziri, N.D., 2009. Niacin ameliorates oxidative stress, inflammation, proteinuria, and hypertension in rats with chronic renal failure. *Am. J. Physiol. Ren. Physiol.* 297, F106–113.
- Citalan-Madrid, A.F., Vargas-Robles, H., Garcia-Ponce, A., Shibayama, M., Betanzos, A., Nava, P., Salinas-Lara, C., Rottner, K., Mennigen, R., Schnoor, M., 2017. Cortactin deficiency causes increased RhoA/ROCK1-dependent actomyosin contractility, intestinal epithelial barrier dysfunction, and disproportionately severe DSS-induced colitis. *Mucosal Immunol.* 10, 1237–1247.
- Elangovan, S., Pathania, R., Ramachandran, S., Ananth, S., Padia, R.N., Lan, L., Singh, N., Martin, P.M., Hawthorn, L., Prasad, P.D., et al., 2014. The niacin/butyrate receptor GPR109A suppresses mammary tumorigenesis by inhibiting cell survival. *Cancer Res.* 74, 1166–1178.
- Elson, C.O., Beagley, K.W., Sharmanov, A.T., Fujihashi, K., Kiyono, H., Tennyson, G.S., Cong, Y., Black, C.A., Ridwan, B.W., McGhee, J.R., 1996. Hapten-induced model of murine inflammatory bowel disease: mucosa immune responses and protection by tolerance. *J. Immunol.* 157, 2174–2185.
- Farrall, R.J., Peppercorn, M.A., 2002. Ulcerative colitis. *Lancet* 359, 331–340.
- Fu, S.P., Li, S.N., Wang, J.F., Li, Y., Xie, S.S., Xue, W.J., Liu, H.M., Huang, B.X., Lv, Q.K., Lei, L.C., et al., 2014. BHBA suppresses LPS-induced inflammation in BV-2 cells by inhibiting NF-kappaB activation. *Mediat. Inflamm.* 2014 (983401).
- Fu, S.P., Wang, J.F., Xue, W.J., Liu, H.M., Liu, B.R., Zeng, Y.L., Li, S.N., Huang, B.X., Lv, Q.K., Wang, W., et al., 2015. Anti-inflammatory effects of BHBA in both in vivo and in vitro Parkinson's disease models are mediated by GPR109A-dependent mechanisms. *J. Neuroinflammation* 12, 9.
- Gambhir, D., Ananth, S., Veeranan-Karmegam, R., Elangovan, S., Hester, S., Jennings, E., Offermanns, S., Nussbaum, J.J., Smith, S.B., Thangaraju, M., et al., 2012. GPR109A as an anti-inflammatory receptor in retinal pigment epithelial cells and its relevance to diabetic retinopathy. *Invest. Ophthalmol. Vis. Sci.* 53, 2208–2217.
- Gao, Z., Yin, J., Zhang, J., Ward, R.E., Martin, R.J., Lefevre, M., Cefalu, W.T., Ye, J., 2009. Butyrate improves insulin sensitivity and increases energy expenditure in mice. *Diabetes* 58, 1509–1517.
- Guilloateau, P., Martin, L., Eeckhaut, V., Ducatelle, R., Zabielski, R., Van Immerseel, F., 2010. From the gut to the peripheral tissues: the multiple effects of butyrate. *Nutr. Rev.* 23, 366–384.
- Guo, Q., Xu, L., Li, H., Sun, H., Wu, S., Zhou, B., 2017. 4-PBA reverses autophagic dysfunction and improves insulin sensitivity in adipose tissue of obese mice via Akt/mTOR signaling. *Biochem. Biophys. Res. Commun.* 484, 529–535.
- Huang, C., Song, P., Fan, P., Hou, C., Thacker, P., Ma, X., 2015. Dietary sodium butyrate decreases Postweaning diarrhea by modulating intestinal permeability and changing the bacterial communities in weaned piglets. *J. Nutr.* 145, 2774–2780.
- Hung, S.P., Sheu, M.J., Ma, M.C., Hu, J.T., Sun, Y.Y., Lee, C.C., Chung, Y.C., Tsai, Y.J., Wang, J.Y., Chen, C.L., 2014. Runx1-deficient afferents impair visceral nociception, exacerbating dextran sulfate-induced colitis. *Brain Behav. Immun.* 35, 96–106.
- Jeong, E.M., Son, Y.H., Choi, Y., Kim, J.H., Lee, J.H., Cho, S.Y., Kim, I.G., 2016. Transglutaminase 2 is dispensable but required for the survival of mice in dextran sulfate sodium-induced colitis. *Exp. Mol. Med.* 48, e267.
- Koh, A., De Vadder, F., Kovatcheva-Datchary, P., Backhed, F., 2016. From dietary fiber to host physiology: short-chain fatty acids as key bacterial metabolites. *Cell* 165, 1332–1345.
- Kostylina, G., Simon, D., Fey, M.F., Yousefi, S., Simon, H.U., 2008. Neutrophil apoptosis mediated by nicotinic acid receptors (GPR109A). *Cell Death Differ.* 15, 134–142.
- Kwon, W.Y., Suh, G.J., Kim, K.S., Kwak, Y.H., 2011. Niacin attenuates lung inflammation and improves survival during sepsis by downregulating the nuclear factor-kappaB pathway. *Crit. Care Med.* 39, 328–334.
- Leonel, A.J., Alvarez-Leite, J.I., 2012. Butyrate: implications for intestinal function. *Curr. Opin. Nutr. and Metab. Care* 15, 474–479.
- Lukasova, M., Malaval, C., Gille, A., Kero, J., Offermanns, S., 2011. Nicotinic acid inhibits progression of atherosclerosis in mice through its receptor GPR109A expressed by immune cells. *J. Clin. Invest.* 121, 1163–1173.
- Ma, X., Fan, P.X., Li, L.S., Qiao, S.Y., Zhang, G.L., Li, D.F., 2012. Butyrate promotes the recovering of intestinal wound healing through its positive effect on the tight junctions. *J. Anim. Sci.* 90 (Suppl. 4), 266–268.
- Macfarlane, S., Macfarlane, G.T., 2003. Regulation of short-chain fatty acid production. *Proc. Nutr. Soc.* 62, 67–72.
- Macia, L., Tan, J., Vieira, A.T., Leach, K., Stanley, D., Luong, S., Maruya, M., Ian McKenzie, C., Hijikata, A., Wong, C., et al., 2015. Metabolite-sensing receptors GPR43 and GPR109A facilitate dietary fibre-induced gut homeostasis through regulation of the inflammasome. *Nat. Commun.* 6, 6734.
- Miller, S.D., Butler, L.D., 1983. T cell responses induced by the parenteral injection of antigen-modified syngeneic cells. I. Induction, characterization, and regulation of antigen-specific T helper cells involved in delayed-type hypersensitivity responses. *J. Immunol.* 131, 77–85.
- Murano, M., Maemura, K., Hirata, I., Toshina, K., Nishikawa, T., Hamamoto, N., Sasaki, S., Saitoh, O., Katsu, K., 2000. Therapeutic effect of intracolonic administered nuclear factor kappa B (p65) antisense oligonucleotide on mouse dextran sulphate sodium (DSS)-induced colitis. *Clin. Exp. Immunol.* 120, 51–58.
- Offermanns, S., 2017. Hydroxy-carboxylic acid receptor actions in metabolism. *Trends Endocrinol. Metab.* 28, 227–236.
- Oppong, G.O., Rapsinski, G.J., Tursi, S.A., Biesecker, S.G., Klein-Szanto, A.J., Goulian, M., McCauley, C., Healy, C., Wilson, R.P., Tukul, C., 2015. Biofilm-associated bacterial amyloids dampen inflammation in the gut: oral treatment with curli fibres reduces the severity of hapten-induced colitis in mice. *NPJ Biofilms and Microbiomes* 1.
- Peterson, L.W., Artis, D., 2014. Intestinal epithelial cells: regulators of barrier function and immune homeostasis. *Nat. Rev. Immunol.* 14, 141–153.
- Piekielna, J., Fichna, J., Janecka, A., 2012. Salvinorin A and related diterpenes—biological activity and potential therapeutic uses. *Postepy Biochem.* 58, 485–491.
- Rahman, M., Muhammad, S., Khan, M.A., Chen, H., Ridder, D.A., Muller-Fielitz, H., Pokorna, B., Vollbrandt, T., Stolting, I., Nadrowitz, R., et al., 2014. The beta-hydroxybutyrate receptor HCA2 activates a neuroprotective subset of macrophages. *Nat. Commun.* 5, 3944.
- Salem, H.A., Wadie, W., 2017. Effect of niacin on inflammation and angiogenesis in a murine model of ulcerative colitis. *Sci. Rep.* 7, 7139.
- Schaubek, M., Clavel, T., Calasan, J., Lagkouvardos, I., Haange, S.B., Jehmlich, N., Basic, M., Dupont, A., Hornef, M., von Bergen, M., et al., 2016. Dysbiotic gut microbiota causes transmissible Crohn's disease-like ileitis independent of failure in antimicrobial defence. *Gut* 65, 225–237.
- Shen, Y., Luo, Q., Xu, H., Gong, F., Zhou, X., Sun, Y., Wu, X., Liu, W., Zeng, G., Tan, N., et al., 2011. Mitochondria-dependent apoptosis of activated T lymphocytes induced by astin C, a plant cyclopeptide, for preventing murine experimental colitis. *Biochem. Pharmacol.* 82, 260–268.
- Simeoli, R., Mattace Raso, G., Pirozzi, C., Lama, A., Santoro, A., Russo, R., Montero-Melendez, T., Berni Canani, R., Calignano, A., Perretti, M., et al., 2017. An orally administered butyrate-releasing derivative reduces neutrophil recruitment and inflammation in dextran sulphate sodium-induced murine colitis. *Br. J. Pharmacol.* 174, 1484–1496.
- Singh, N., Gurav, A., Sivaprakasam, S., Brady, E., Padia, R., Shi, H., Thangaraju, M., Prasad, P.D., Manicassamy, S., Munn, D.H., et al., 2014. Activation of Gpr109a, receptor for niacin and the commensal metabolite butyrate, suppresses colonic inflammation and carcinogenesis. *Immunity* 40, 128–139.
- Sivaprakasam, S., Prasad, P.D., Singh, N., 2016. Benefits of short-chain fatty acids and their receptors in inflammation and carcinogenesis. *Pharmacol. Ther.* 164, 144–151.
- Soga, T., Kamohara, M., Takasaki, J., Matsumoto, S., Saito, T., Ohishi, T., Hiyama, H., Matsuo, A., Matsushime, H., Furuichi, K., 2003. Molecular identification of nicotinic acid receptor. *Biochem. Biophys. Res. Commun.* 303, 364–369.
- Sun, Y., Wu, X.X., Yin, Y., Gong, F.Y., Shen, Y., Cai, T.T., Zhou, X.B., Wu, X.F., Xu, Q., 2010. Novel immunomodulatory properties of cirsiineol through selective inhibition of IFN-gamma signaling in a murine model of inflammatory bowel disease. *Biochem. Pharmacol.* 79, 229–238.
- Taggart, A.K., Kero, J., Gan, X., Cai, T.Q., Cheng, K., Ippolito, M., Ren, N., Kaplan, R., Wu, K., Wu, T.J., et al., 2005. (D)-beta-Hydroxybutyrate inhibits adipocyte lipolysis via the nicotinic acid receptor PUMA-G. *J. Biol. Chem.* 280, 26649–26652.
- Thangaraju, M., Cresci, G.A., Liu, K., Ananth, S., Gnanaprakasam, J.P., Browning, D.D., Mellinger, J.D., Smith, S.B., Digby, G.J., Lambert, N.A., et al., 2009. GPR109A is a G-protein-coupled receptor for the bacterial fermentation product butyrate and functions as a tumor suppressor in colon. *Cancer Res.* 69, 2826–2832.
- Tunaru, S., Kero, J., Schaub, A., Wufka, C., Blaukat, A., Pfeffer, K., Offermanns, S., 2003. PUMA-G and HM74 are receptors for nicotinic acid and mediate its anti-lipolytic effect. *Nat. Med.* 9, 352–355.
- Ungaro, R., Mehandru, S., Allen, P.B., Peyrin-Biroulet, L., Colombel, J.F., 2017. Ulcerative colitis. *Lancet* 389, 1756–1770.
- Wanders, D., Graff, E.C., White, B.D., Judd, R.L., 2013. Niacin increases adiponectin and decreases adipose tissue inflammation in high fat diet-fed mice. *PLoS One* 8, e71285.
- Wise, A., Foord, S.M., Fraser, N.J., Barnes, A.A., Elshourbagy, N., Eilert, M., Ignar, D.M., Murdock, P.R., Steplewski, K., Green, A., et al., 2003. Molecular identification of high and low affinity receptors for nicotinic acid. *J. Biol. Chem.* 278, 9869–9874.
- Worthington, J.J., Reimann, F., Gribble, F.M., 2017. Enterendocrine cells—sensory sentinels of the intestinal environment and orchestrators of mucosal immunity. *Mucosal Immunol.* 11, 3–20.
- Xu, X., Lin, S., Chen, Y., Li, X., Ma, S., Fu, Y., Wei, C., Wang, C., Xu, W., 2017. The effect of metformin on the expression of GPR109A, NF-kappaB and IL-1beta in peripheral blood leukocytes from patients with type 2 diabetes mellitus. *Ann. Clin. Lab. Sci.* 47, 556–562.
- Yang, S., Li, X., Wang, N., Yin, G., Ma, S., Fu, Y., Wei, C., Chen, Y., Xu, W., 2015. GPR109A expression in the murine Min6 pancreatic Beta cell line, and its relation with glucose metabolism and inflammation. *Ann. Clin. Lab. Sci.* 45, 315–322.
- Zandi-Nejad, K., Takakura, A., Jurewicz, M., Chandraker, A.K., Offermanns, S., Mount, D., Abdi, R., 2013. The role of HCA2 (GPR109A) in regulating macrophage function. *FASEB J.* 27, 4366–4374.
- Zhang, L., Du, J., Yano, N., Wang, H., Zhao, Y.T., Dubielecka, P.M., Zhuang, S., Chin, Y.E., Qin, G., Zhao, T.C., 2017. Sodium butyrate protects against high fat diet-induced cardiac dysfunction and metabolic disorders in type II diabetic mice. *J. Cell. Biochem.* 118, 2395–2408.